Probing the moisture-induced drug recrystallization in hydroxypropyl methylcellulose-based amorphous solid dispersions

Carbohydrate Polymers 388 (2026) 125580

Contents lists available at ScienceDirect

Carbohydrate Polymers

journal homepage: www.elsevier.com/locate/carbpol

Probing the moisture-induced drug recrystallization in hydroxypropyl methylcellulose-based amorphous solid dispersions☆

Arvindh Seshadri Suresh [a,b], Famke Van Brempt [a], Susanna Abrahmsén-Alami [b,c], Anette Larsson [a,b,d,*]

[a] Department of Chemistry and Chemical Engineering, Chalmers University of Technology, 41296, Gothenburg, Sweden
[b] FibRe Centre for Lignocellulose-based Thermoplastics, Department of Chemistry and Chemical Engineering, Chalmers University of Technology, SE-41296, Gothenburg, Sweden
[c] Pharmaceutical Technology & Development, Operations, AstraZeneca, Gothenburg, Sweden
[d] Wallenberg Wood Science Centre, Chalmers University of Technology, Gothenburg, 41296, Sweden

ARTICLE INFO

Keywords:
Amorphous solid dispersions
Hydroxypropyl methylcellulose
Hot melt extrusion
Water sorption
Drug recrystallization
Naproxen

ABSTRACT

Hydroxypropyl methylcellulose (HPMC), a widely used cellulose derivative, plays a central role in stabilizing drug-containing amorphous solid dispersions (ASDs), by inhibiting the drug recrystallization. However, the moisture sorption behavior of HPMC can compromise the physical stability of ASDs under humid conditions. This study examines how humidity, drug loading, storage time, and spatial location within the ASD together influence the recrystallization behavior of a model drug (naproxen) in HPMC-based ASDs prepared via hot melt extrusion. We hypothesized that moisture induced drug recrystallization is governed primarily by the water sorption characteristics of HPMC. To investigate moisture induced drug recrystallization, extrudates were stored for 14 days at 75% and 98% RH. All formulations remained fully amorphous (>99.5%) at 75% RH, whereas significant recrystallization occurred at 98% RH. Notably, recrystallization initiated at the extrudate surface, reflecting moisture driven structural gradients within the polymer matrix. These results establish a structure–property relationship linking HPMC hydration and increased chain mobility to drug recrystallization, providing a mechanistic insight relevant for designing robust moisture-resistant cellulose derivatives-based drug delivery systems.

1. Introduction

Oral administration of drugs has been the most prominent route of drug administration and constitutes almost 60% of the market, owing to its convenient nature, simplicity in handling and storage, cost-effectiveness, and independent administration of the drugs by the patients (Deac et al., 2023; Govender, Kissi, Larsson, & Tho, 2021). An important property that orally administered drugs should possess is dissolution in the gastrointestinal fluids and permeation through the gut membrane. The Biopharmaceutical classification system (BCS), established in 1995 by Amidon et al. (Amidon, Lennernäs, Shah, & Crison, 1995) classifies drugs according to their solubility and permeability characteristics, with Type II and IV drugs (high/low permeability and low solubility) garnering significant attention, as poor aqueous solubility can lead to reduced bioavailability (BA) (Baghel, Cathcart, & O'Reilly, 2016; Yazdi, Benson, Taylor, & Edgar, 2025).

For drugs where the solubility of the crystalline form is too low and the desired BA cannot be obtained through micronization or use of nanoparticles, amorphous solid dispersions (ASDs) are one way to overcome the solubility challenges. In ASDs the amorphous drug is dispersed in the polymeric phase (Kissi et al., 2021), and the presence of the polymer matrix increases the physical stability of the drug in its amorphous state by inhibiting its recrystallization (Bapat, Paul, Tseng, & Taylor, 2024; Shi, Li, Yeh, Wang, & Xin, 2020). The polymer matrices employed are crucial to the performance of the ASDs, and their selection matched to the drug substance characteristics plays a major role in the performance of the ASDs. Among the different polymers employed, the cellulose derivative hydroxypropyl methylcellulose (HPMC) has been found to be a suitable polymeric carrier in ASDs, likely because the two different substituents attached to the carbohydrate polymer chain offer

☆ This article is part of a Special issue entitled: 'EPNOE 2025' published in Carbohydrate Polymers.

* Corresponding author at: Department of Chemistry and Chemical Engineering, Chalmers University of Technology, 41296, Gothenburg, Sweden.
E-mail address: anette.larsson@chalmers.se (A. Larsson).

https://doi.org/10.1016/j.carbpol.2026.125580
Received 5 March 2026; Received in revised form 4 June 2026; Accepted 17 June 2026
Available online 23 June 2026

Table 1
Physicochemical properties of AFFINISOL™ HPMC HME 100LV.

MeO[a] (wt%)	DS_{avg}[b]	HPO[a] (wt%)	MS_{avg}[b]	Total Substitution[a] (%)	MeO/HPO ratio[a]	Molecular weight, M_w (kDa)[c]	T_g (°C)
22.0–27.0	1.91	25.0–32.0	0.91	47.0–59.0	0.89	190.1 ± 2.6	101.15 ± 0.35

[a] Information from the manufacturer, Dow Chemical Co. limits.
[b] Calculated with MeO (wt%) and HPO (wt%) using eq. 5. in (Viridén, Wittgren, & Larsson, 2009).
[c] Measured as duplicates using Size-exclusion chromatography (Refer Section SI1.)

opportunities for interactions with drug molecules (Barba, d'Amore, Chirico, Lamberti, & Titomanlio, 2009; Chang et al., 2020; Fan et al., 2018; Jin et al., 2023; Sarabu et al., 2020; J. Zhang et al., 2017; X. Zhang et al., 2025). The balance of methoxy and hydroxypropyl groups dictates water uptake, which modulates polymer chain mobility and thereby influences the likelihood of drug recrystallization. This structure–property relationship forms the basis for the present study (Larsson, Viridén, Stading, & Larsson, 2010; Otoni, Lorevice, Moura, & Mattoso, 2018).

While there are different methods to prepare ASDs, hot melt extrusion (HME) has proven to be a successful manufacturing process owing to its environmental friendliness, ability to perform continuous manufacturing, solvent-free nature, and potential for industrial-level scale-up (Ha et al., 2025; Keßler et al., 2025; Patil et al., 2024; Sarabu et al., 2020; Sarode et al., 2014). Recent developments have also enabled HPMC to be processed with ease using HME. A new grade of HPMC was introduced by Dow Chemicals, specially designed for this purpose, a few years ago (Huang et al., 2016). This grade, called the AFFINISOL™ HPMC HME, has garnered considerable attention owing to its ease of extrudability, thermal stability and ability to stabilize the drug in ASDs (Larsen, Kissi, Nogueira, Genina, & Tho, 2024; Mora-Castaño et al., 2024; Prasad et al., 2019; Vlad et al., 2025).

ASDs are thermodynamically in a metastable state, which gives rise to a potential risk of physical instability through recrystallization of the drug (Guan et al., 2021). Recrystallization is further accelerated by environmental factors such as relative humidity (RH) (Pajzderska, Mielcarek, & Wąsicki, 2022). Several studies have investigated the effect of humidity on the physical stability of ASDs experimentally (Bhujbal et al., 2021; Chen et al., 2018; Feng et al., 2016; Haku, Suzuki, Ohashi, Titapiwatanakun, & Fukami, 2025; Konno & Taylor, 2008; Li et al., 2020; Lin et al., 2018; O'Connell et al., 2025; Rumondor, Wikström, Van Eerdenbrugh, & Taylor, 2011; Tian et al., 2014; Wu & Van Mooter, 2023; S. Zhang, Lee, & Chow, 2019; Zhao et al., 2024). In particular, Taylor and co-workers (Marsac et al., 2010; Marsac, Konno, Rumondor, & Taylor, 2008; Purohit & Taylor, 2015, 2017; Rumondor, Marsac, Stanford, & Taylor, 2009) have studied extensively how relative humidities (or moisture) affects the phase behavior and physical stability of ASDs. Xie and Taylor (Xie & Taylor, 2017) analyzed the stability of ASDs prepared with celecoxib and different polymers such as PVP, PVPVA, and HPMC acetate succinate (HPMCAS), by exposing them to elevated temperatures and relative humidities. The results suggested that under high-humidity environments, ASDs with stronger drug-polymer interactions and lower moisture sorption were resistant to moisture-induced phase separation and drug recrystallization. Purohit and Taylor studied the phase behavior (Purohit & Taylor, 2017) and phase separation kinetics (Purohit & Taylor, 2015) of ritonavir-based ASDs with PVP, PVPVA and HPMCAS upon exposure to high humidities and bulk water (during dissolution). They observed amorphous-amorphous phase separation (AAPS) for ritonavir-PVP and ritonavir-PVPVA based ASDs upon high RH storage and dissolution. This was attributed to the preferential interaction of the polymer with water that led to disruption of drug-polymer interaction and subsequent formation of drug-rich phase. Rumondor et al. (Rumondor, Stanford, & Taylor, 2009) investigated the influence of polymer type (PVP and HPMCAS) and storage RH on crystallization kinetics of felodipine-based ASDs. It was observed that above 75% RH, crystallization of felodipine occurred at a higher rate in PVP-based ASDs than HPMCAS-based ASDs and this was associated with the highest propensity of PVP to absorb water and result in moisture-induced drug-polymer immiscibility. However, the majority of studies focus on ASDs with excipients consisting of synthetic polymers such as PVP, PVPVA, or specifically HPMCAS when the focus is on cellulose derivatives. Thus, there seems to be a lack of studies that analyze the combined influence of storage humidity, storage times, and drug loading on physical stability/drug recrystallization in HPMC based ASDs and correlate the behavior of HPMC under moisture exposure to the drug recrystallization phenomena.

Beyond their functional role in stabilizing amorphous drugs, cellulose-based polymers such as HPMC are derived from renewable resources, making them attractive for designing environmentally responsible pharmaceutical formulations. Improved understanding of their moisture driven behavior therefore also contributes to more sustainable drug delivery strategies.

With these details in mind, the primary objective of the study was to understand how storage humidity (and hence, water uptake), storage time, and drug loading influence the drug recrystallization in HPMC based ASDs and further elucidate the underlying mechanisms. The hypothesis of the study is that drug recrystallization is primarily governed by the moisture sorption characteristics of HPMC, the interactions occurring between moisture and HPMC, and the resultant enhancement in its polymer chain mobilities. To test this, ASDs were prepared with AFFINISOL™ HPMC HME 100LV as the excipient and a model drug (naproxen) at drug loadings from 5 to 30 wt%, using hot melt extrusion. The characteristics of the ASDs were evaluated using differential scanning calorimetry (DSC), Fourier transform infrared (FT-IR) spectroscopy, and wide-angle X-ray scattering (WAXS). Furthermore, to investigate moisture-induced drug recrystallization, the ASDs were stored at 75% and 98% RH for 14 days and analyzed at regular intervals using the aforementioned techniques.

2. Materials and methods

2.1. Materials

AFFINISOL™ HPMC HME 100 LV (100 cP) was kindly donated by Dow Wolff Cellulosics GmbH, Walsrode, Germany. The physicochemical properties of HPMC HME 100LV used in the current study are given in Table 1. Further, a model drug, naproxen (Molecular weight = 230.26 g/mol), was purchased as a powder form from MP Biomedicals, United States. The salts, sodium chloride and potassium sulfate, were purchased from Sigma Aldrich. All chemicals were of analytical grade and used without further purification procedures.

2.2. Methods

2.2.1. Thermogravimetric analysis

Thermogravimetric analysis (TGA) of neat materials (HPMC HME 100LV and naproxen powders) was conducted to assess thermal stability and guide the selection of processing conditions for hot melt extrusion. TGA was carried out using a Mettler Toledo TGA/DSC 3+ Thermal Analysis System. The powders were weighed into a 70 μL alumina crucible and heated from 25 to 500 °C with a heating rate of 10 °C/min in a nitrogen atmosphere.

2.2.2. Preparation of HPMC/naproxen amorphous solid dispersions

The preparation of the ASDs was performed using a twin-screw Haake Minilab II (Thermo Fisher Scientific) micro compounder. HPMC HME 100LV and naproxen were initially pre-mixed into a physical mixture at different drug loadings (5, 10, 20, and 30 wt%) using a mortar and pestle. The physical mixture was subsequently fed into the micro compounder and extruded into filaments through a 2 mm circular die. The extrusion process was carried out at 170 °C and 90 rpm. The extruded filaments were stored in zip-lock bags and used for further characterization without any post-processing steps. Samples with 5, 10, 20 and 30 wt% naproxen loading are named as HPMC + NAP5, HPMC + NAP10, HPMC + NAP20 and HPMC + NAP30, respectively, throughout the article.

2.2.3. Physical stability test

Extrudates of pure HPMC HME 100LV and ASDs were subjected to a physical stability test by storing them at room temperature (23 °C) in two different desiccators with varying relative humidities (RHs). The selected RHs were 75% and 98%. Saturated NaCl solution and K_2SO_4 solution were used to obtain 75% RH and 98% RH, respectively. The samples were stored for 14 days. At regular intervals of storage, samples from the desiccator were removed and analyzed using calorimetric, spectroscopic, and scattering techniques to examine changes induced by storage humidity and time.

2.2.4. Differential scanning calorimetry

Differential scanning calorimetry (DSC) was carried out using a Mettler Toledo DSC 5+ system. DSC was performed on the neat materials (in powder form), as well as the ASDs (in extrudate form), before and during the physical stability test. The samples were weighed in a 40 μL aluminum pan and sealed with a lid containing a pinhole to allow the escape of volatile substances. All measurements were conducted in a nitrogen atmosphere with a gas flow of 50 mL/min.

Before the physical stability test, the extrudate samples were measured as duplicates from −40 to 225 °C, at 10 °C/min (heating and cooling rates), and the glass transition temperature (T_g) was estimated from the second heating curves. The DSC measurements of HPMC HME 100LV and naproxen powders were, on the other hand, performed over the temperature range 25 to 200 °C at 10 °C/min (heating and cooling rate).

In addition to measuring the T_g of the ASDs experimentally, Gordon-Taylor (GT) equation (Gordon & Taylor, 1952) was used to calculate the theoretical T_g:

$$T_{g,theoretical} = \frac{w_1 \bullet T_{g1} + k \bullet w_2 \bullet T_{g2}}{w_1 + k \bullet w_2} \quad (1)$$

where w_1, T_{g1}, and w_2, T_{g2}, are the weight fraction and glass transition temperatures of naproxen and HPMC HME 100LV, respectively. The glass transition temperature of naproxen was taken as 5 °C from literature (Löbmann et al., 2011). The parameter k in the original GT equation derived for polymer blends represented the uneven contribution of free volume of the individual components to the T_g of the blend (Kalogeras & Brostow, 2009). However, in the context of ASDs, k refers to the interaction density between the drug and polymer and can be estimated from the following equation (Iyer et al., 2021):

$$k = \frac{\rho_1 \bullet T_{g1}}{\rho_2 \bullet T_{g2}} \quad (2)$$

where ρ_1 and ρ_2 are the densities of naproxen (=1.25 g/cm^3) (Paudel, Van Humbeeck, & Van Den Mooter, 2010) and HPMC HME 100LV (=1.2 g/cm^3) (Iemtsev et al., 2020), respectively.

Furthermore, DSC was performed during the physical stability test to evaluate changes in the T_g with storage time and humidity. For these measurements, the stored extrudates (as duplicates) were analyzed on the 7th and 14th day of storage. The samples were heated at 10 °C/min from starting temperatures ranging between −75 to −30 °C, to end temperatures between 60 and 100 °C, depending on the sample. The T_g was evaluated from the first heating curves.

2.2.5. Wide-angle X-ray scattering

Wide-angle X-ray scattering (WAXS) measurements were performed to analyze the stability of the ASDs and monitor the drug recrystallization during the physical stability test, using a Mat: Nordic X-ray scattering instrument (SAXSLAB), equipped with a high brilliance Rigaku 003 X-ray micro-focus, Cu-Kα radiation source (λ = 1.5406 Å) and a Pilatus 300 K detector. The instrument calibration was performed using lanthanum hexaboride (LaB_6). The exposure time during the measurement was 300 s. The measurements were performed using an ambient sample holder for neat materials (in powder form) and ASDs stored in ambient conditions. On the other hand, a sandwich cell with Kapton windows was used to characterize ASDs subjected to physical stability tests. The data for the samples measured using the sandwich cell were corrected for the background by subtracting the signal from the Kapton windows. The WAXS curves were plotted and analyzed using OriginPro 2023.

The percentage of recrystallized drug was calculated from the WAXS curves using the following equation:

$$Percentage\ of\ recrystallized\ drug\ (\%) = \frac{Area\ under\ peaks\ arising\ from\ crystalline\ drug}{Total\ area\ under\ the\ WAXS\ curve} * 100 \quad (3)$$

2.2.6. Fourier transform infrared spectroscopy

Fourier transform infrared (FT-IR) spectroscopy of the neat materials (powders), and the ASDs (extrudates) were conducted using the Bruker Vertex70v spectrometer in the attenuated total reflectance (ATR) mode. The measurements were performed in the wavenumber range 4000–400 cm^{-1}, with 32 scans and a resolution of 4 cm^{-1} (average of 3 spectra). Furthermore, they were baseline-corrected using an adaptive baseline correction algorithm and normalized to the 1049 cm^{-1}, the C—O stretching band in the HPMC. For samples, where the 1049 cm^{-1} band was not clear due to the presence of strong peaks from the drug, the spectra were normalized at the 1026 cm^{-1} band of naproxen. The data processing was performed using Spectragryph 1.2.16.1 software (Menges, 2022), while the spectra were plotted using OriginPro 2023.

2.2.7. Water uptake study

A water uptake study was conducted to quantify the amount of water that ASDs absorbed during storage in humid environments. At time intervals similar to the physical stability tests, the samples (in duplicates) were removed from the desiccators, weighed using a Mettler Toledo AE163 Analytical Balance, and then placed back. Further, the data was plotted as water content vs storage time (average). The error was calculated as the difference divided by 2.

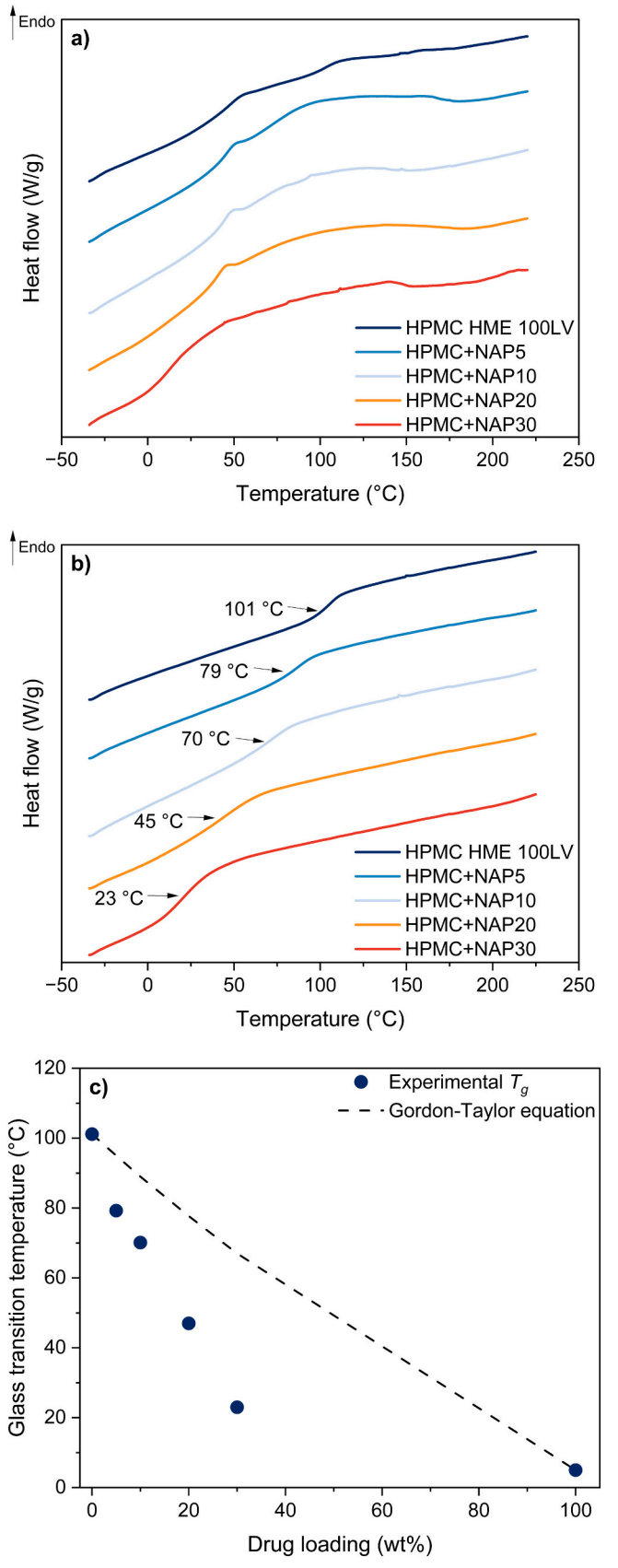

Fig. 1. DSC thermograms of HPMC HME 100LV and HPMC + NAP ASDs, a) First heating, b) Second heating, c) Experimental, and theoretical T_g calculated using eq. 1, of the ASDs.

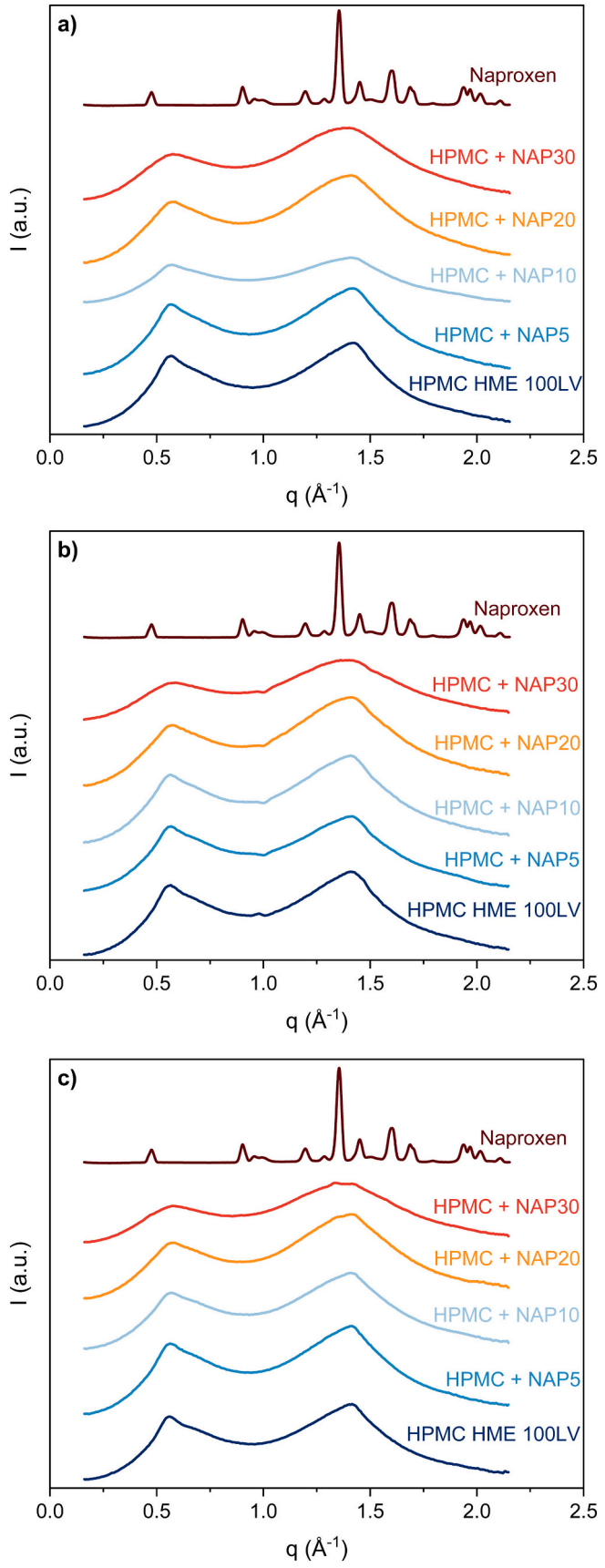

Fig. 2. WAXS curves of HPMC HME 100LV, naproxen, and HPMC + NAP ASDs, a) After extrusion, b) After 2 months of storage, c) After 6 months of storage.

3. Results and discussion

3.1. Characterization of HPMC HME 100LV, naproxen, and their ASDs

3.1.1. Thermogravimetric analysis

Extrudates of HPMC HME 100LV and HPMC/naproxen ASDs were manufactured using HME, a process conducted at elevated temperatures. Therefore, TGA was performed on HPMC HME 100LV and naproxen powders to evaluate the thermal stability of the materials and determine the extrusion temperature. The TGA thermograms of HPMC HME 100LV and naproxen are shown in Fig. SI1. From the thermograms, it is evident that HPMC HME 100LV and naproxen show good thermal stability up to 325 °C and 215 °C, respectively. However, it should be noted that thermal processing of AFFINISOL™ HPMC HME grades have shown to be prone to discoloration and degradation even at temperatures around 200 °C (Svoboda et al., 2023). Therefore, based on literature evidence, the supplier's recommendation, and the TGA results, an extrusion temperature of 170 °C was adopted for the extrusion of the ASDs.

3.1.2. Differential scanning calorimetry

The DSC thermograms of HPMC HME 100LV and naproxen powder are shown in Fig. SI2. In the second heating curve, HPMC HME 100LV exhibits a clear glass transition at 100 °C. This is similar to the T_g of 103 °C obtained by Gupta et al. (Gupta, Solanki, & Serajuddin, 2016). Furthermore, pure naproxen powder exhibited a distinct melting peak at 158 °C in the first heating curve and a melting peak at 157 °C in the second heating curve.

DSC studies of the ASDs were conducted to assess 1) the plasticization effect of naproxen on HPMC HME 100LV, 2) whether naproxen was in the amorphous state and 3) the miscibility of naproxen in HPMC HME 100LV, across all drug loadings. The DSC thermograms (first and second heating) of HPMC HME 100LV and the ASDs are displayed in Fig. 1a and b, respectively. Furthermore, the experimentally determined T_g and theoretical T_g calculated using the Gordon-Taylor equation (eq. 1), of the ASDs are shown in Fig. 1c. The T_g of the drug plotted in Fig. 1c was obtained from literature (Löbmann et al., 2011).

The glass transition temperatures of the ASDs were calculated from the second heating curves due to the presence of a faint (and broad) peak between 50 and 60 °C in the first heating curves that made it difficult to evaluate the T_g for certain samples (HPMC + NAP10 and HPMC + NAP20). The broad peak is likely due to the loss of residual moisture and/or enthalpy relaxation in the samples after extrusion. Nevertheless, T_g estimated for the remaining samples from the first heating were similar to the values obtained from the second heating (Table SI1), indicating no major influence in the T_g due to the first heating run.

The DSC measurements of the ASDs do not show any melting peak for naproxen across all drug loadings. Additionally, a single T_g is observed for all the samples. On comparing the experimental T_g values with theoretical values obtained through the Gordon-Taylor equation (eq. 1), it is observed that the experimental T_g values undergo a negative deviation. This indicates that the drug-polymer interactions are weaker compared to the interactions present in the individual components (Péter-Haraszti et al., 2024). Similar results have been obtained by Pugliese et al.(Pugliese et al., 2021) and Wang et al. (Wang, Rades, & Grohganz, 2023) for HPMCAS- Acetaminophen and HPMC-Carbamazepine ASD systems. The negative deviation from the predicted T_g was attributed to the domination of intramolecular interactions between like species.

Furthermore, glass transition temperatures measured for the ASDs indicate that the addition of naproxen results in plasticization effect on the HPMC HME 100LV carrier. Li et al. (B. Li, Konecke, Wegiel, Taylor, & Edgar, 2013) demonstrated the plasticization effect of curcumin on HPMCAS, whereas Kissi et al. (Kissi et al., 2021) reported a similar effect of naproxen on Kollidon® VA 64. The presence of a single T_g along with the absence of melting peaks from the drug indicates that naproxen is molecularly dispersed in the HPMC HME 100LV carrier at all drug loadings.

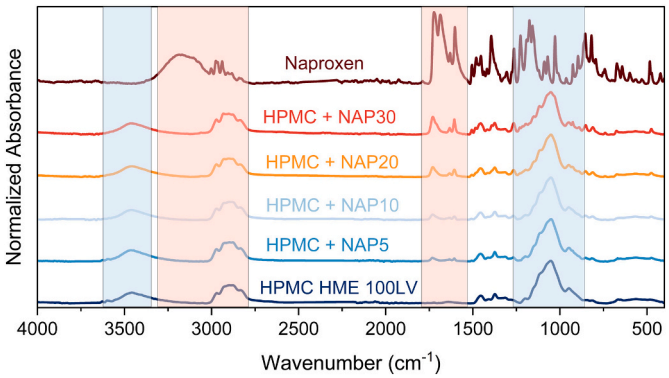

Fig. 3. FT-IR spectra of HPMC HME 100LV, naproxen, and their ASDs. Measurements of ASDs were performed on extrudate's cross-section.

3.1.3. Wide-angle X-ray scattering

WAXS measurements were performed to check whether naproxen remained in the amorphous state in the ASDs across all drug loadings. Furthermore, to ensure the long-term stability of the ASDs, the measurements were carried out at three time points: after extrusion, after 2 months, and after 6 months of storage under ambient conditions (samples stored in zip-lock bags). The WAXS profiles of HPMC HME 100LV, naproxen, and HPMC + NAP ASDs are shown in Fig. 2. The naproxen sample was measured in powder form, whereas the measurements for HPMC HME 100LV and HPMC + NAP ASDs were performed on extrudates.

From the WAXS profiles, it is evident that, after extrusion, all ASD samples exhibit signals similar to HPMC HME 100LV, with no peaks corresponding to the crystalline drug. In addition, the incorporation of drug leads to the broadening of the peaks at q = 0.57 $Å^{-1}$ and q = 1.4 $Å^{-1}$. These results indicate that we have successfully prepared ASDs of HPMC HME 100LV and naproxen. Furthermore, on storage of the ASDs at ambient conditions, naproxen remained in an amorphous state in the majority of the samples even after 6 months, as seen from the absence of any drug peaks. The only exception was HPMC + NAP30, which exhibited faint drug peaks after 6 months of storage. On using eq. 3, the percentage of recrystallized drug was evaluated to be around 0.1%, indicating that the crystalline fraction is not substantial. Hence, it can be concluded that HPMC + NAP ASDs predominantly exhibit long-term stability (up to 6 months) when stored at ambient conditions.

3.1.4. Fourier transform infrared spectroscopy

FT-IR spectroscopy was performed to analyze the intermolecular interactions between HPMC HME 100LV and naproxen at different drug loadings. The FT-IR spectra of HPMC HME 100LV and naproxen powders are shown in Fig. SI3, while FT-IR spectra of HPMC HME 100LV extrudate, naproxen, and the HPMC + NAP ASDs are displayed in Fig. 3. In addition, Fig. SI4 shows a zoomed-in version of Fig. 3 focusing on the wavenumber range 1500–1800 cm^{-1}. These spectra represent measurements performed on the extrudate cross-section. The highlighted orange regions predominantly indicate characteristic bands from naproxen, and the blue regions indicate bands from HPMC HME 100LV. This is followed in all the IR spectra shown throughout the article.

The FT-IR spectrum of HPMC HME 100LV shows characteristic bands that serve as a fingerprint of the different chemical groups present. The band at 1049 cm^{-1} corresponds to the C—O stretching vibration, while that at 1118 cm^{-1} points towards the C-O-C pyranose ring vibration, and the band at 1456 cm^{-1} is associated with C—H bending. Furthermore, bands between 2800 and 3000 cm^{-1} correspond to C—H stretching, and the band at 3458 cm^{-1} arises from O—H bond stretching (Vlad et al.,

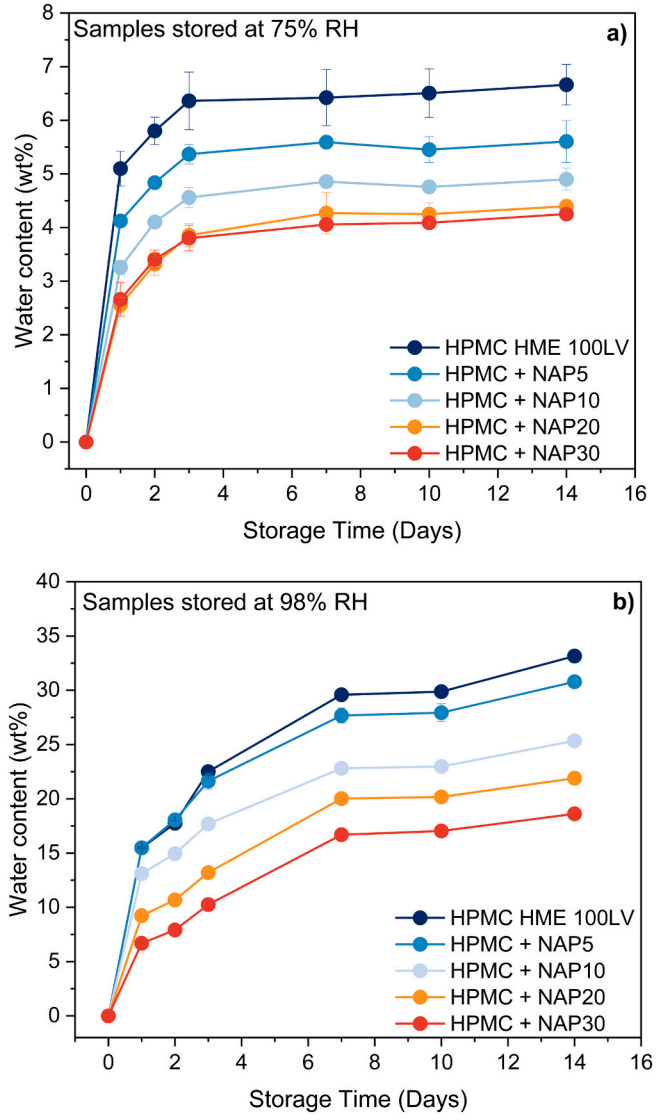

Fig. 4. Water sorption isotherms of HPMC HME 100LV and ASDs stored at, a) 75% RH, b) 98% RH. Error bars in Fig. 4b are small and hence, not visible clearly.

2025).

The most representative bands of crystalline naproxen are found at 1681 and 1724 cm^{-1}, which correspond to the carbonyl stretching of the carboxylic group. The band at 1681 cm^{-1} refers to the hydrogen-bonded carbonyl group, while the band at 1724 cm^{-1} refers to the free carbonyl group. If naproxen is converted to its amorphous state, the IR spectra will undergo certain shifts. The hydrogen-bonded carbonyl band shifts to 1697 cm^{-1}, while the free carbonyl band moves to 1728 cm^{-1} (Löbmann et al., 2011, 2013). Furthermore, the broad band between wavenumbers 3100 and 3200 cm^{-1} is associated with O—H stretching of the carboxylic acid group (Liu, Zhou, & Zhang, 2017)(Paudel & Van Den Mooter, 2012).

The FT-IR spectra of the HPMC + NAP ASDs exhibited the characteristics bands of both HPMC HME 100LV and naproxen. However, the ASD preparation led to two dominant changes in the spectral features. Firstly, it can be observed in the spectra (Fig. 3 and Fig. SI4) that the intense band at 1681 cm^{-1} corresponding to the hydrogen-bonded carbonyl group has undergone a significant reduction in intensity and shifted to a higher wavenumber of 1706 cm^{-1}. This is a clear indication of disruption of hydrogen bonding between naproxen molecules (Paudel & Van Den Mooter, 2012) and can be viewed more clearly in Fig. SI4, where a shoulder is observed at 1706 cm^{-1}. Secondly, the band attributed to the non-hydrogen bonded carbonyl group (band at 1724 cm^{-1}) undergoes a reduction in intensity as well and shifts to 1730 cm^{-1}. These reductions in intensities and shifts in the characteristic bands upon the preparation of the ASDs with HPMC HME 100LV, seem to indicate the disruption of interactions between naproxen molecules and formation of new intermolecular interactions with HPMC HME 100LV, which facilitates the amorphous nature of the ASDs.

3.2. Physical stability test

3.2.1. Water uptake

Water uptake measurements were performed to quantify the water absorbed by the ASDs as a function of storage humidity and time. Fig. 4 shows the sorption isotherms for the ASDs stored at 75% and 98% RH.

The primary observation for both humidities is the decrease in water sorption as drug loading increases. This is due to naproxen's greater hydrophobicity, which increases the overall hydrophobicity of the samples relative to HPMC HME 100LV. Samples stored at 75% RH reach a plateau on the 3rd day and absorb approximately 6.5 wt% of water (HPMC HME 100LV) after 14 days.

In contrast, all samples stored at 98% RH absorb substantial amounts of water; for instance, HPMC HME 100LV and HPMC + NAP30 absorb approximately 33 wt% and 18 wt% water, respectively, after 14 days of storage. Moreover, the water uptake does not reach equilibrium for any of the samples, unlike samples stored at 75% RH. However, it should be noted that when the authors measured water uptake after 3 weeks of storage (data not shown), the samples had reached an equilibrium water content corresponding to ~33 wt%, ~30 wt%, ~26 wt%, ~22 wt%, and ~ 18 wt% for HPMC HME 100LV, HPMC + NAP5, HPMC + NAP10, HPMC + NAP20 and HPMC + NAP30, respectively.

3.2.2. Wide-angle X-ray scattering

The physical stability and the drug recrystallization phenomenon of HPMC + NAP ASDs were primarily monitored using WAXS measurements. The WAXS profiles of HPMC + NAP ASDs exposed to 75 and 98% RH are shown in Fig. 5. The figure illustrates how the WAXS profile of each sample changes with storage humidity and storage time.

When the ASDs are stored at 75% RH (WAXS curves in the left column in Fig. 5), it can be observed that, irrespective of the drug loading, the prepared ASDs do not exhibit any WAXS peaks that correspond to the crystalline naproxen even after 14 days of storage. Furthermore, the ASDs at different storage times and drug loadings show WAXS profiles similar to HPMC HME 100LV. However, on careful inspection, the WAXS profile of HPMC + NAP30 exhibited very small peaks at q = 1.4 $Å^{-1}$. Using eq. 3, the percentage of recrystallized drug was found to be less than 0.2%, making it negligible. Therefore, it can be concluded that HPMC + NAP ASDs exhibit good physical stability on storing at 75% RH for the storage periods investigated in the current study.

On the contrary, the HPMC + NAP ASDs that were exposed to 98% RH show a striking difference in their characteristics based on the drug loading. The sample with 5 wt% naproxen exhibits WAXS characteristics similar to those of the samples stored at 75% RH, with no evidence of drug recrystallization. This indicates the amorphous nature of the sample, even under high-humidity conditions. On the other hand, the sample with 10 wt% naproxen shows signs of peaks arising from crystalline naproxen. In addition, samples with 20 and 30 wt% naproxen exhibit strong WAXS peaks corresponding to naproxen at different storage times. Fig. 6 shows the storage time at which drug recrystallization was identified for each ASD stored at 98% RH, and the calculated percentage of recrystallized drug (using eq. 3) for each ASD across different storage times.

It can be observed that samples with 10, 20, and 30 wt% naproxen exhibit the onset of drug recrystallization on Day 10, Day 7, and Day 2 of storage, respectively. On increasing the storage time, the intensity of drug recrystallization increases irrespective of the drug loading. This can

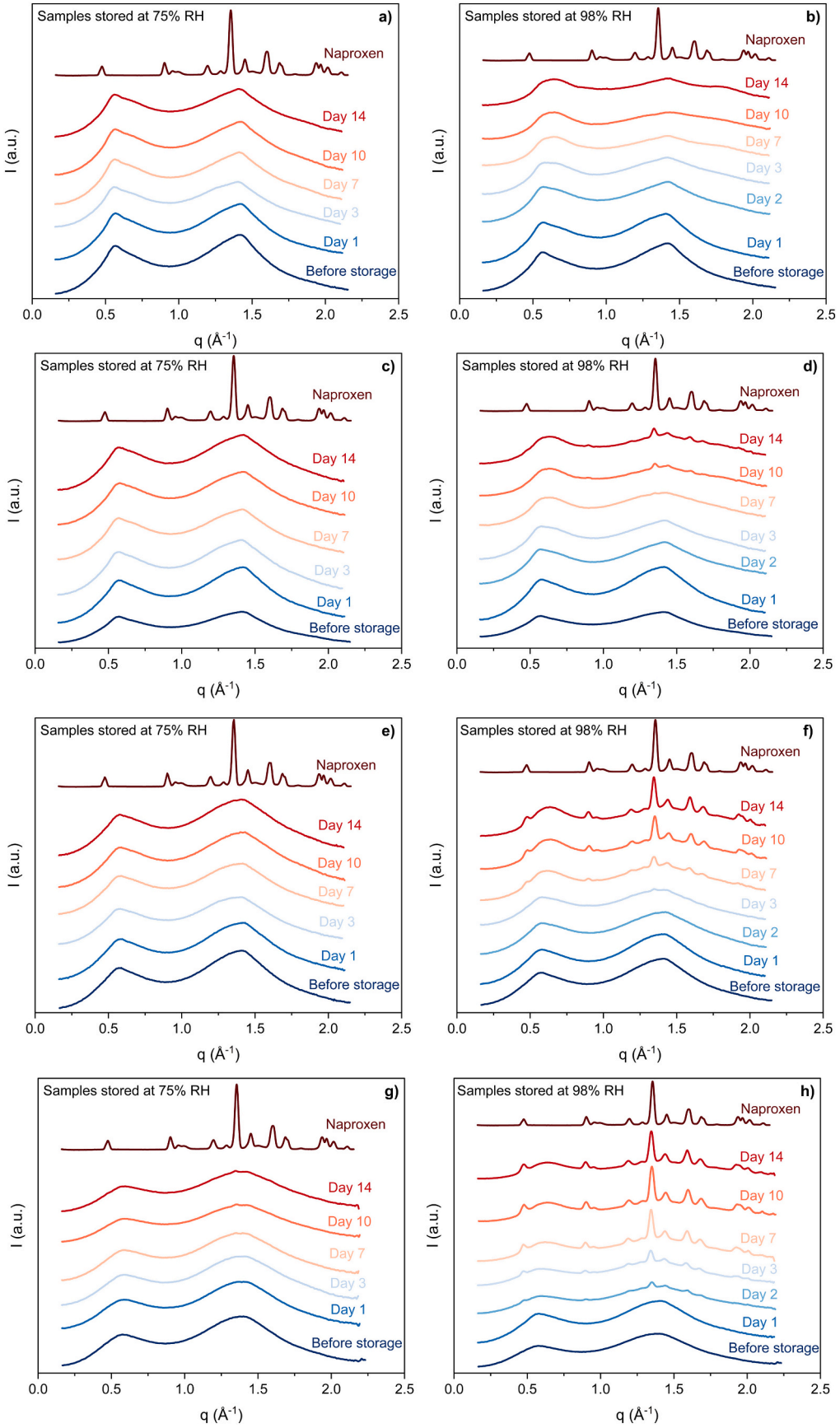

Fig. 5. WAXS profiles of HPMC + NAP ASDs stored at different humidities, HPMC + NAP5 ((a) 75% RH, (b) 98% RH), HPMC + NAP10 ((c) 75% RH, (d) 98% RH), HPMC + NAP20 ((e) 75% RH, (f) 98% RH), HPMC + NAP30 ((g) 75% RH, (h) 98% RH). The y-axis (intensities) is offset to enable stacking of the curves.

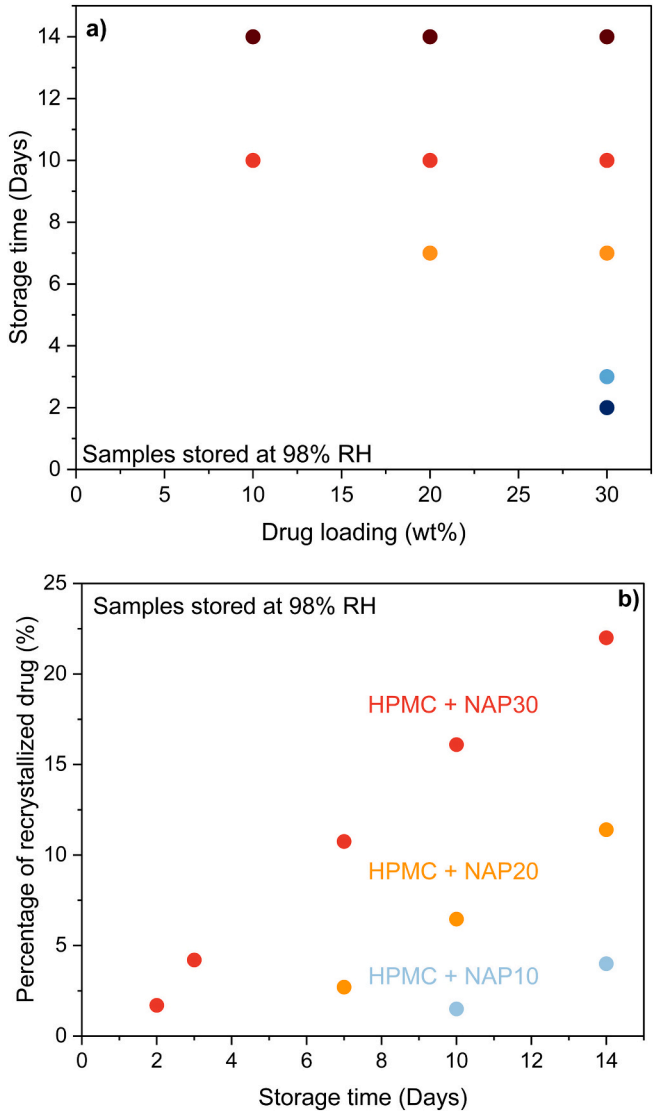

Fig. 6. a) Time of drug recrystallization for samples stored at 98% RH, b) Percentage of recrystallized drug for samples stored at 98% RH.

be viewed in Fig. 6b, where the percentage of recrystallized drug increases with storage time. Furthermore, HPMC + NAP30 exhibits the highest percentage of recrystallized drug, followed by HPMC + NAP20 and HPMC + NAP10. In addition to the percentage of recrystallized drug, the apparent crystallization rates were determined by using a linear fit to the data in Fig. 6b and estimating the slope. The apparent crystallization rates for HPMC + NAP10, HPMC + NAP20, and HPMC + NAP30 were 0.6%/day, 1.2%/day, and 1.8%/day, respectively, showing a linear increase with drug loading.

3.2.3. *Fourier transform infrared spectroscopy*

FT-IR measurements were performed on the cross-section of the extrudates, as well as the surface and core of the extrudates. The schematic illustrating the sample preparation of FT-IR measurements is shown in Fig. 7. The spectra obtained from cross-sections of extrudates of ASDs stored at 75% and 98% RH are presented in Fig. SI5 and Fig. 8, respectively. The spectra shown correspond to samples measured on Day 7 and Day 14 of storage.

The samples stored at 75% RH show no pronounced changes in their IR spectra, regardless of drug loading. The bands corresponding to the amorphous naproxen centered at approximately 1730 cm^{-1} remain unchanged with storage at all concentrations. Similarly, the peaks arising from the drug between the wavenumbers 1600 and 1630 cm^{-1} remain as well upon storage at 75% RH. The only noticeable change for the samples stored at 75% RH is a slight increase in the intensity of the peak at 1730 cm^{-1}. Nevertheless, the spectra indicate the amorphous nature of the drug after 14 days of storage and the absence of any drug recrystallization in the bulk of the extrudates.

On the contrary, the fingerprint region between 1575 cm^{-1} and 1775 cm^{-1} showed differences among the samples stored at 98% RH. For all ASDs, there were no strong drug-associated peaks visible in this region, as was seen for the samples stored at 75% RH. This is primarily due to the high moisture absorption by the ASDs at 98% RH. The high moisture absorption is witnessed by the appearance of a new band at around 1650 cm^{-1} in the samples stored at 98% RH. The band at 1650 cm^{-1} arises from hydrogen bonding between HPMC HME 100LV and water molecules, and represents the H-O-H angle-bending vibrations (Cichosz & Masek, 2020). The presence of this band potentially masks the bands from the drug in this region. Another interesting observation is the increase in intensity of the band at 3420 cm^{-1} and the presence of a shoulder at 3275 cm^{-1} across all ASDs. Both these bands arise from the hydroxyl groups present in HPMC HME 100LV. The band at 3420 cm^{-1} represents the intramolecular hydrogen bonding of O(2)H---O(6), while the shoulder at 3275 cm^{-1} corresponds to the intermolecular hydrogen bonding of O(6)H---O(3) (Oh, Yoo, Shin, & Seo, 2005). Furthermore, the band at 3420 cm^{-1} has shifted from 3458 cm^{-1} after storage, which can be reasoned as the weakening of intramolecular hydrogen bonding in HPMC HME 100LV. This result, along with the increase in band intensity, indicates that at high relative humidity, there is an interaction between water and the hydroxyl groups of HPMC HME 100LV (which act as sorption centers) through hydrogen bonding (Kalutskaya & Gusev, 1980). Additionally, no significant changes in the drug-related bands were observed after storage at 98% RH, as measured on extrudate cross-sections.

In addition to measuring the extrudate cross-section, IR measurements were performed on the core and surface of the extrudates as aforementioned. The corresponding IR spectra of HPMC + NAP20 and HPMC + NAP30, stored at 75% and 98% RH for 14 days, are shown in Fig. 9. Furthermore, the IR spectra for HPMC + NAP 5 and HPMC + NAP10 are shown in Fig. SI6. For the measurements performed on the extrudate surface, the IR penetration depth (in ATR setup) was calculated based on eq. 1. in (Grdadolnik, 2002) and found to be in the range 0.6–2.5 μm.

On examining the figures, it is apparent that the storage of the ASDs gives rise to distinct spectral features in measurements performed on the extrudate surface and core. The surface of HPMC + NAP20 and HPMC + NAP30, stored at 75% and 98% RH, show a higher proportion of bands corresponding to the crystalline drug. For samples stored at 98% RH, the bands at 1681 cm^{-1} and 1724 cm^{-1}, which are attributed to the hydrogen-bonded and non-hydrogen-bonded carbonyl groups in crystalline naproxen, appear indicating the crystallization of naproxen on the extrudate surface upon exposure to moisture. Furthermore, on comparing samples stored in 75% and 98% RH, it is evident that samples stored at 75% RH exhibit fewer and lower-intensity drug peaks. This effect of humidity is seen clearly for HPMC + NAP10, where strong drug-associated bands such as the characteristic bands at 1681 cm^{-1} and 1724 cm^{-1} are visible only on the extrudate surface for samples stored at 98% RH.

On the other hand, the core of all ASDs, regardless of drug concentration and humidity, shows similar features to samples measured prior to storage. The only differences are observed for samples stored at 98% RH, where a new band is visible at approximately 1650 cm^{-1}, and the intensity of the 3420 cm^{-1} band has increased. These relate to the water absorption of the samples as elucidated in the previous paragraphs. These indicate that storing the ASDs under humid conditions has led to preferential crystallization of the drug on the extrudate surface (refer to Fig. SI7 for visual photographs) rather than in the bulk/core of the extrudate. In addition, migration of drug molecules from the bulk of the

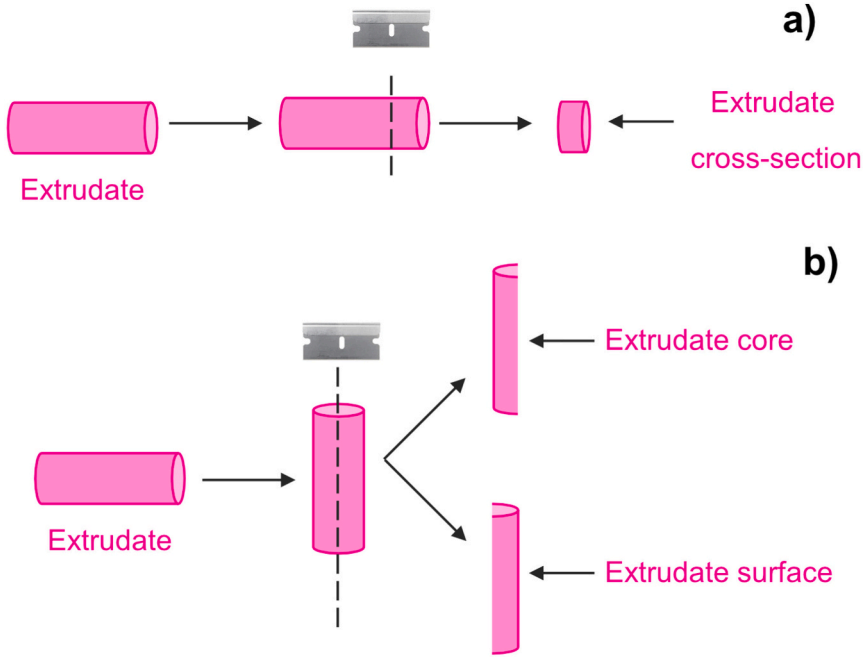

Fig. 7. Schematic of sample preparation for FT-IR measurements on, a) cross-section of extrudates, b) surface and core (interior) of extrudates.

extrudates to the surface also occurs and is discussed in the next section.

3.2.4. Moisture-enhanced molecular mobility of the ASD systems

From the results reported above, it is evident that relative humidity and, thus, moisture has a significant effect on the drug recrystallization in ASDs. One of the major factors influencing the stability of ASDs is the system's molecular mobility, which changes upon exposure to moisture. This led the authors to elucidate the changes in the molecular mobility of the HPMC + NAP systems as a function of storage humidity and time. To study this, DSC measurements were performed, and the changes that occurred in the T_g of the ASDs upon storage at 75% and 98% RH were investigated. The measurements were performed on Day 7 and Day 14 of storage. The T_g as a function of drug loading is shown in Fig. 10, while the corresponding DSC thermograms are shown in Fig. SI8.

The change in T_g with storage coincides with the water-uptake and drug recrystallization observed in the ASDs. For samples stored at 75% RH, water uptake was low, ranging from 4 to 7 wt% depending on the sample. This water uptake led to a reduction in T_g of around 40 °C for HPMC HME 100LV and 20 °C for HPMC + NAP30. Despite a reduction in T_g, most samples (up to 20 wt% of naproxen) remained in a glassy state when stored at room temperature. This indicates relatively low molecular mobility in the ASD system and maybe one reason why samples stored at 75% RH remained amorphous.

On the other hand, samples stored at 98% RH exhibited a significant reduction in T_g. After 7 days of storage, all samples, including the HPMC HME 100LV extrudate, exhibited a similar T_g (−25 to −35 °C). This large reduction arises from the high amounts of water uptakes by HPMC HME 100LV and the ASDs. Furthermore, after 14 days of storage, the water uptake was only slightly higher than on Day 7; hence, the T_g values are also superimposed. Another observation noticed for samples stored at 98% RH is the independence of T_g values on drug loading, compared to samples stored at 75% RH where it was dependent. This phenomenon will be further discussed in the next section. To conclude, the significant decrease in T_g (at 98% RH) is an indication of high molecular mobility of the ASD system and is caused by the water sorption, which is majorly driven by the polymeric excipient. Thus, the moisture-enhanced molecular mobility may be one of the primary driving forces behind the observed drug recrystallization.

3.3. Deeper insights into the influence of moisture in ASDs

Amorphous solids exhibit higher solubility and dissolution rates compared to the crystalline form, while simultaneously suffering from thermodynamic instability (tendency to recrystallize) owing to their higher free volume and molecular mobility (Taylor & Zografi, 2025). To eliminate the instability issues, stabilizing excipients are added to prepare dosage forms of amorphous drugs. In the current work, HPMC HME 100LV has been used as an excipient to form solid dispersions and stabilize the drug in the amorphous state. In traditional formulations, HPMC serves as a matrix and is generally used to achieve extended-release performance. Upon hydration, it swells rapidly and continuous exposure to water leads to the gradual hydration of the matrix towards the core, resulting in three distinct zones: an outer gel layer, a swollen glassy layer, and an inner dry core (Barba et al., 2009; Bin, Joshi, & Lam, 2009). The gel-layer formation process is commonly attributed to Case II swelling (Caccavo et al., 2017), where the rate-limiting factor is the rate of polymer chain relaxation.

HPMC HME 100LV is selected as the ASD carrier due to being specifically designed for processing via HME. During formation and in the dry state, it effectively stabilizes the amorphous state of the drug when stored in ambient conditions up to at least six months of storage, as indicated by the WAXS results (Fig. 2). Although HPMC has proof of being capable of stabilizing the amorphous state upon moisture exposure (J. Li, Wang, & Yu, 2023; Riekes et al., 2014; J. Zhang, Shi, & Tao, 2023), the balance between the HPMC hydrophilicity and the specific HPMC-drug interaction is critical for its capability of inhibiting recrystallization.

In this study, ASDs of HPMC HME 100LV and naproxen were prepared at different drug loadings (0–30 wt%). Upon preparation, all the samples remained in an amorphous state as seen from absence of melting peak of crystalline drug from DSC results (Fig. 1) as well as crystalline drug peaks in the WAXS profiles (Fig. 2). In addition, the samples also exhibited a single T_g, ruling out the possibility of AAPS in the ASD systems. Furthermore, the aim of the study was to investigate how the recrystallization of the drug was influenced by different factors such as storage humidity (and thus, water uptake), storage time and drug loading in ASD systems where HPMC is used as an excipient.

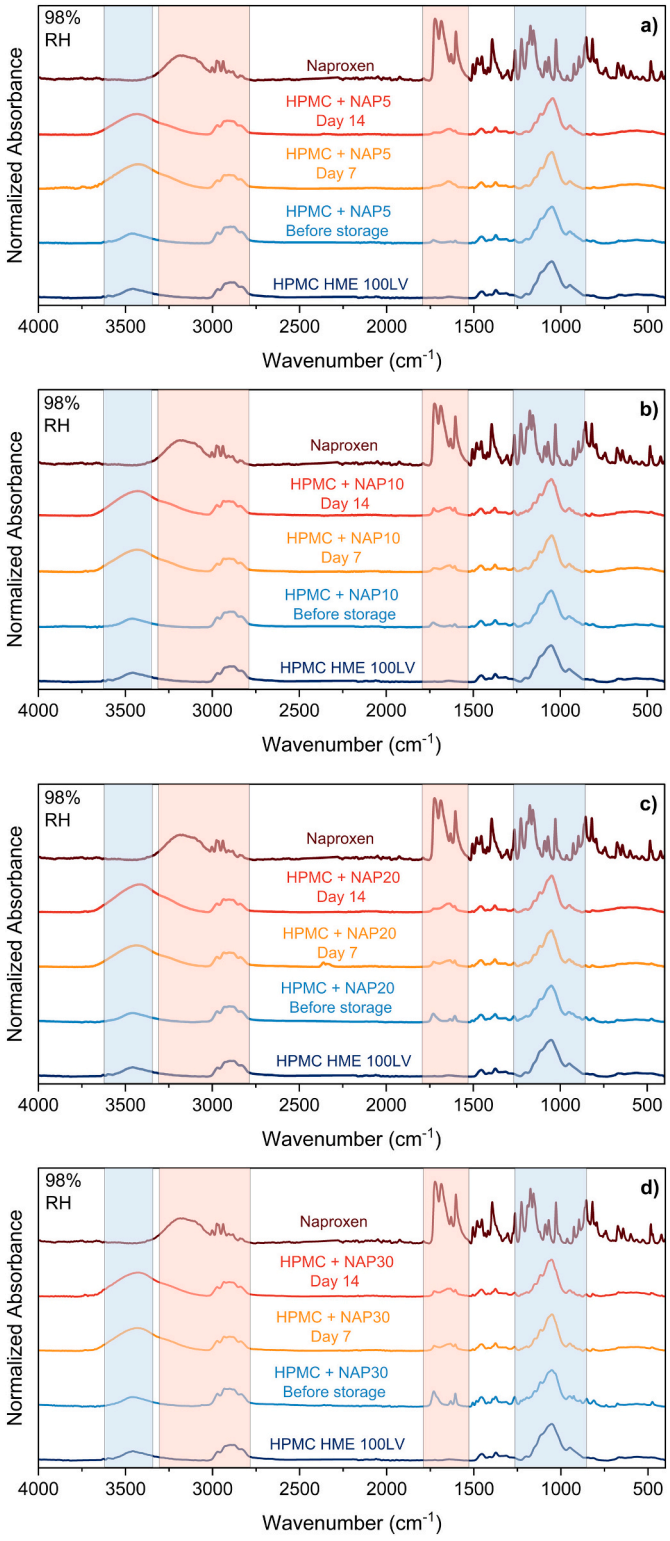

Fig. 8. FT-IR spectra of ASDs (measured on cross-section) stored at 98% RH (a) HPMC + NAP5, b) HPMC + NAP10, c) HPMC + NAP20, d) HPMC + NAP30.

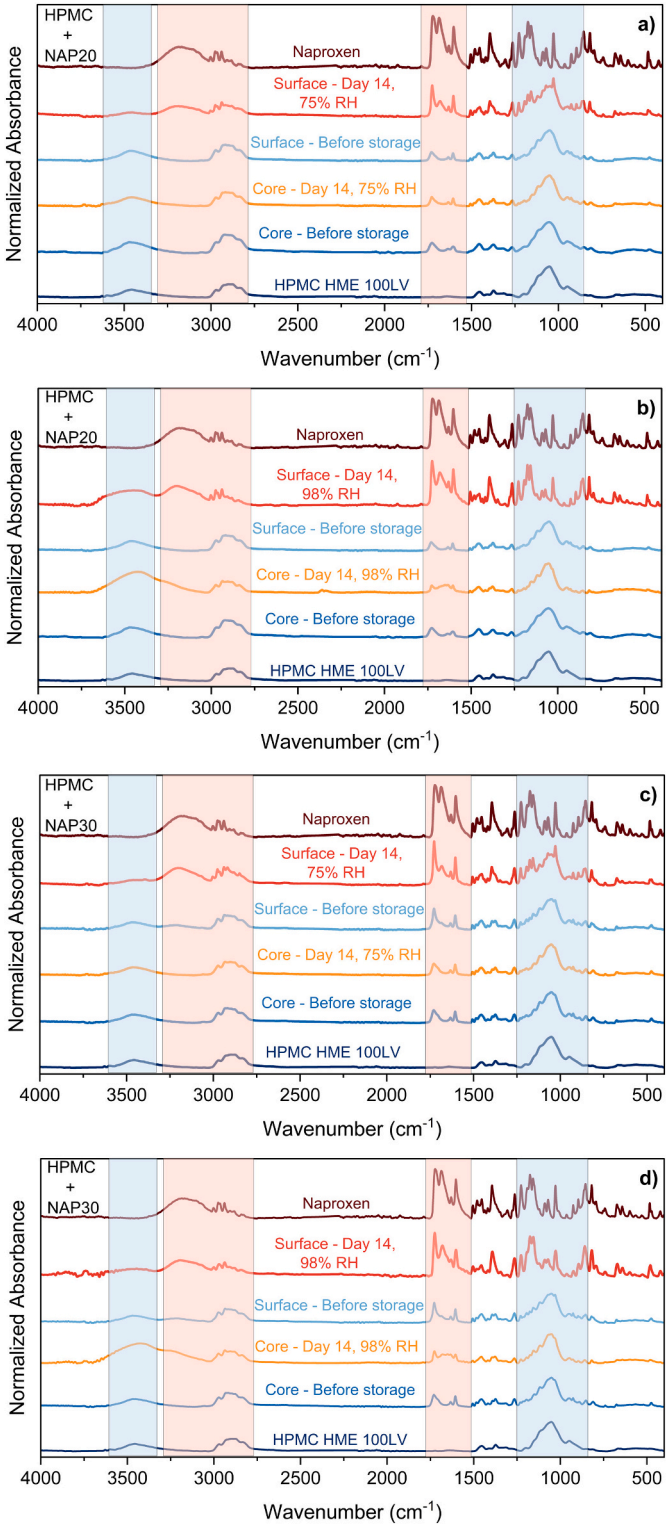

Fig. 9. FT-IR spectra from the core and surface of ASDs stored at 75% RH (a) HPMC + NAP20, c) HPMC + NAP30, and 98% RH (b) HPMC + NAP20, d) HPMC + NAP30.

3.3.1. Behavior of ASD upon moisture exposure

In ASD's the formation of drug crystals usually occurs through nucleation and crystal growth (Moseson & Taylor, 2023; J. Zhang et al., 2024). The drug molecules in the ASDs need to interact with each other first to form a nucleus. Factors that facilitate enhanced interactions of drug molecules include a higher probability that individual drug molecules encounter one another in the ASD system. The higher probability is caused by (i) molecular mobility of the drug, which is influenced by polymer chain mobility and strength of polymer-drug interactions, (ii) drug loading (as confirmed with higher crystallization rates observed for higher drug loadings, Fig. 6b).

When ASD extrudates are exposed to moisture, the authors hypothesize that they follow a moisture sorption mechanism similar to the

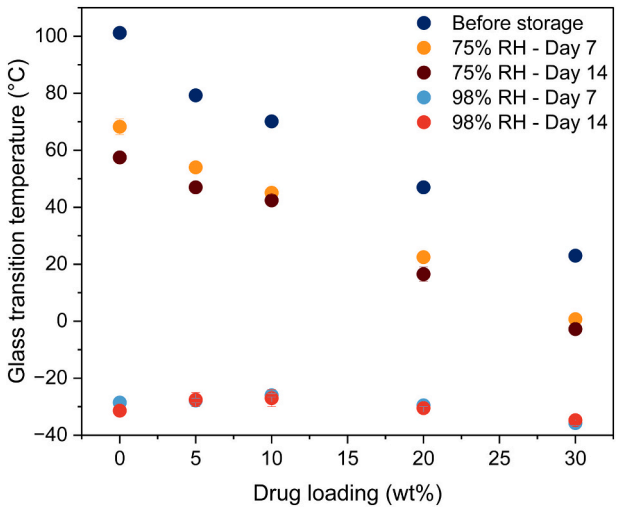

Fig. 10. Glass transition temperatures of the ASDs before and after storage.

hydration mechanism of HPMC. Thus, the water penetrates from the surface into the interior. The high-humidity environment, i.e., 98% RH in the current study (where drug recrystallization was observed, see Fig. 5 and Fig. 6), led to the ASDs absorbing large amounts of water (refer Fig. 4). The water sorption of the ASD system is governed by the ways in which HPMC HME 100LV interacts and takes up water, as it is the hydrophilic component and its concentration is dominant in the ASD. Furthermore, the impact of water on the mobility of HPMC chains becomes important and dictates the behavior of the ASD system. In the current study, water sorption resulted in the significant lowering of the T_g (see Fig. 10), which indicates an appreciable increase in the polymer chain mobility and free volume, thereby enabling higher drug mobility (i.e., mobility of free naproxen molecules). In addition, another phenomenon was observed where the T_g of samples stored at 75% RH depend on the drug loading, whereas the T_g for those stored at 98% RH was independent. In samples stored at 75% RH, the drug predominantly remained in the amorphous state, as seen from WAXS results (Fig. 5). Hence, the drug contributes to a plasticization effect leading to lower T_g with increasing drug loading. On the contrary, most samples stored at 98% RH exhibited significant drug recrystallization, resulting in lower amounts of amorphous drug in the ASDs. The crystalline drug is not molecularly dispersed and does not contribute to the plasticization of the ASDs. Therefore, the reduction in T_g is primarily controlled by water and HPMC–water interactions.

As aforementioned, the enhancement of mobility in ASD upon moisture exposure is determined by interactions between water and HPMC HME 100LV. In the present work, the formation of chemical interactions in the form of intermolecular hydrogen bonding between water and HPMC HME 100LV was observed from the IR results. This manifested as the appearance of a new band at 1650 cm^{-1} and the shifting of the band at 3420 cm^{-1} from 3458 cm^{-1} (Fig. 8). In the dry state or at low amounts of moisture, HPMC HME 100LV and naproxen exhibited interactions (even if they may be weakly interacting) and this is one of the reasons for naproxen to remain amorphous. However, on exposure to high moisture levels, the strength of HPMC–water interactions are higher than HPMC–naproxen interactions. Furthermore, analysis using the Gordon-Taylor equation (Fig. 1c) suggested a negative deviation of the observed single experimental T_g (before storage), which indicates stronger interactions between the individual components (polymer–polymer and drug–drug) compared to the weaker polymer–drug interactions. The reduced polymer-drug interactions at high moisture levels, in combination with the hydrophobicity of naproxen, cause the moisture-induced drug recrystallization to occur.

The mechanism of moisture-induced drug recrystallization process, as explained by nucleation and growth phenomena (see Fig. 11) requires sufficient mobility of free naproxen molecules. It is imperative for the naproxen molecules to be able to diffuse within the ASD system to form nuclei and grow into crystals. This is facilitated by the enhancement in polymer chain mobility governed by the water uptake and polymer relaxation, thus being the rate-limiting step for moisture-induced drug recrystallization in ASDs.

An implication of the current study is to gain a better understanding of the storage conditions for the HPMC-naproxen ASDs that will ensure long-term physical stability. A rule-of-thumb is the T_g – 50 rule, which indicates that the storage temperature must be 50 °C below the sample's T_g to ensure stability (Hancock, Shamblin, & Zografi, 1995; Moseson & Taylor, 2023). In the current study, the storage temperature for samples stored at 75% RH was close to their T_g or within the range of 50 °C. Despite this, they exhibited good stability under the investigated time period. However, these results alone cannot be used to suggest storage conditions that will ensure long-term stability of the ASDs. It is imperative to carry long-term stability studies spanning 1–2 years at different storage humidities or computational prediction studies to determine the storage conditions. Nevertheless, the T_g – 50 rule can be used as a good starting point given the knowledge of T_g of the ASDs after exposure to moisture.

3.3.2. *Surface crystallization in ASDs*

Another interesting observation is that the ASDs, upon storage in humid conditions, showed a higher fraction of drug crystals on the extrudate surface, as proven by the presence of strong characteristic bands of crystalline naproxen in the IR spectra (particularly at 1681 cm^{-1} and 1724 cm^{-1}, see Fig. 9 and Fig. SI6). Prior to storage, IR measurements indicated, within the detection limit, a homogeneous distribution of drug molecules in most samples, although HPMC + NAP30 exhibited a slight surface enrichment of the drug. This is illustrated in Fig. 9, which shows that the HPMC + NAP30 surface exhibits more drug-associated bands than the core. This could have arisen from the flow profile during extrusion, and has been previously observed for

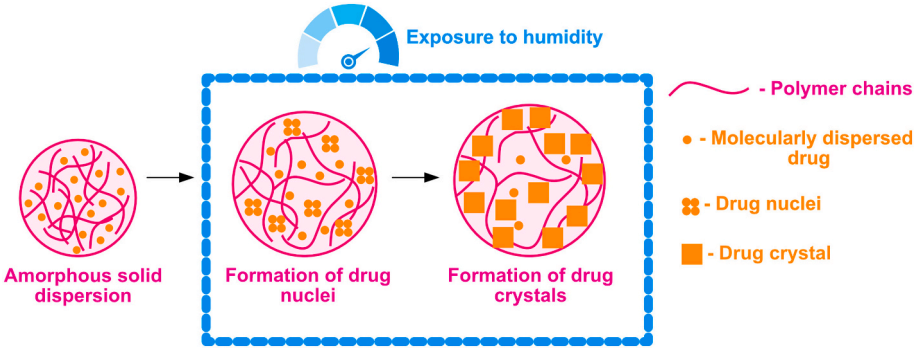

Fig. 11. Schematic of the mechanism of drug recrystallization upon exposure to moisture/humidity in ASD systems.

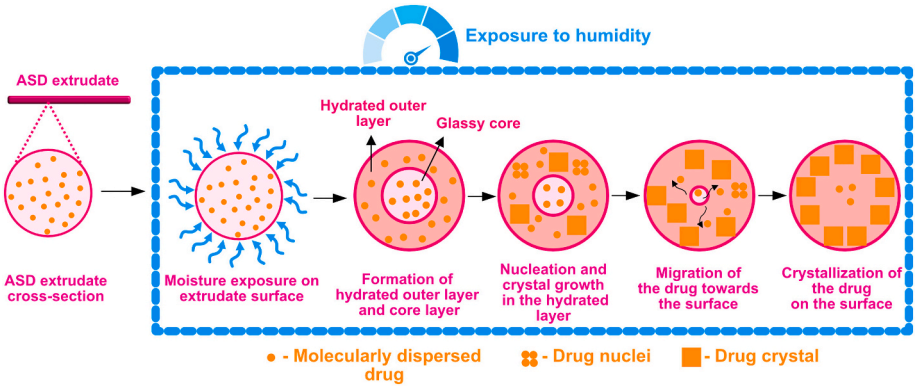

Fig. 12. Schematic on the mechanism of migration and crystallization of the drug on extrudate surface upon exposure to moisture/humidity.

ASDs prepared using HME (Deshmukh et al., 2020; Windbergs, Strachan, & Kleinebudde, 2009; Yang et al., 2014).

The phenomenon of enrichment of crystals at the extrudate surface upon moisture exposure can be explained by the water sorption characteristics of HPMC HME 100LV. When the ASDs are exposed to moisture during storage (75% and 98% RH), the water sorption begins at the extrudate surfaces initially and further penetrates to the interior. This leads to the extrudate surface experiencing significantly greater moisture exposure than the bulk, thus forming a hydrated outer layer and a glassy (and dry) core. The HPMC–naproxen interactions remained unaffected and a proportion of drug remained amorphous in the extrudate core under the investigated time period. This can be observed from the absence of any characteristic peak shifts in the IR spectrum when measured on the cross-section/core of the extrudates (Fig. 8 and Fig. 9). As aforementioned, two correlated phenomena are suggested to occur primarily in the hydrated outer layer:

(i) disruption of HPMC–naproxen interactions due to stronger HPMC–water interactions.
(ii) enhanced mobility of HPMC HME 100LV chains due to water sorption, enabling higher mobility of free naproxen molecules.

The free drug molecules in the hydrated layer (and close to the surface) will begin to undergo nucleation and grow into crystals. As water penetrates further into the extrudate, the hydrated layer increases enabling higher proportion of drug crystals to be formed. The formation of drug crystals depletes drug molecules near the crystal surface, creating a concentration gradient with lower concentrations near the crystal and higher concentrations farther away (in the inner regions). This acts as a driving force to the migration of drug molecules towards the surface and the migration is primarily enabled by the moisture-enhanced polymer mobility. This process continues throughout the storage period leading to an increasing proportion of drug crystals on the extrudate surface with time. A schematic illustrating the mechanism of the drug's surface crystallization on exposure to moisture/humidity is shown in Fig. 12.

4. Conclusion

This work provides a comprehensive understanding of moisture-induced drug recrystallization in HPMC based ASDs prepared via hot melt extrusion. The study highlights the critical role of environmental humidity, storage duration, and drug loading in determining the physical stability of ASDs. While formulations retained their amorphous character (>99.5%) under ambient and moderate humidity conditions, exposure to high humidity (98% RH) resulted in significant drug recrystallization during the investigated time period (14 days), underscoring the vulnerability of ASDs to moisture.

Water sorption in these systems followed a mechanism analogous to HPMC hydration, characterized by the formation of a hydrated outer layer and a progressively shrinking dry core. This structural evolution was accompanied by a marked reduction in T_g to values below room temperature, indicating enhanced molecular mobility. Increased mobility facilitates drug diffusion and nucleation, which are prerequisites for crystallization. Infrared spectroscopy further revealed that moisture promotes strong HPMC–water interactions at the expense of HPMC–naproxen interactions, weakening the stabilizing polymer–drug interaction and enabling naproxen molecules to reorganize into crystalline domains.

Crystallization was observed to initiate at the extrudate surface rather than the core, driven by higher moisture exposure at the surface and subsequent drug migration. The formation of crystals creates local depletion zones, establishing concentration gradients that act as driving forces for continued drug migration and crystal growth. Furthermore, drug loading played an important role with drug recrystallization rates scaling with drug loading, indicating higher proportion of drug have a higher probability of interacting with other drug molecules and undergoing the recrystallization process. The observations from this study emphasize the importance of the excipient's behavior under moisture exposure in dictating the drug recrystallization. These insights have practical implications for the development of physically stable ASDs, highlighting the need for robust moisture protection strategies, such as optimized packaging, humidity-controlled storage, and potential incorporation of moisture scavengers. Understanding these mechanisms in detail can guide formulators in designing ASDs with improved resistance to environmental stress, thereby ensuring long-term stability and therapeutic performance.

CRediT authorship contribution statement

Arvindh Seshadri Suresh: Writing – review & editing, Writing – original draft, Visualization, Validation, Methodology, Investigation, Formal analysis, Data curation, Conceptualization. **Famke Van Brempt:** Methodology, Investigation, Formal analysis, Data curation. **Susanna Abrahmsén-Alami:** Writing – review & editing, Writing – original draft, Supervision, Resources, Project administration. **Anette Larsson:** Writing – review & editing, Writing – original draft, Supervision, Resources, Project administration, Funding acquisition, Conceptualization.

Declaration of competing interest

The authors declare that they have no known competing financial interests or personal relationships that could have appeared to influence the work reported in this paper.

Acknowledgements

The authors would like to thank the Swedish Research Council (Grant number: 2022-04352) for funding this research as well as the support from "FibRe – a Competence Center for Design for Circularity: Lignocellulose Based Thermoplastics", partly funded by the Swedish Innovation Agency *V*INNOVA (2019-00047). This work was performed in part (FT-IR and WAXS measurements) at the Chalmers Materials Analysis Laboratory, CMAL. Giovanni Tizzanini is acknowledged for the help with SEC measurements.

Appendix A. Supplementary data

Supplementary data to this article can be found online at https://doi.org/10.1016/j.carbpol.2026.125580.

Data availability

Data will be made available on request.

References

Amidon, G. L., Lennernäs, H., Shah, V. P., & Crison, J. R. (1995). A theoretical basis for a biopharmaceutic drug classification: The correlation of in vitro drug product dissolution and in vivo bioavailability. *Pharmaceutical Research, 12,* 413–420. https://doi.org/10.1023/A:1016212804288

Baghel, S., Cathcart, H., & O'Reilly, N. J. (2016). Polymeric amorphous solid dispersions: A review of Amorphization, crystallization, stabilization, solid-state characterization, and aqueous Solubilization of biopharmaceutical classification system class II drugs. *Journal of Pharmaceutical Sciences, 105*(9), 2527–2544. https://doi.org/10.1016/j.xphs.2015.10.008

Bapat, P., Paul, S., Tseng, Y. C., & Taylor, L. S. (2024). Interplay of drug-polymer interactions and release performance for HPMCAS-based amorphous solid dispersions. *Molecular Pharmaceutics, 21*(3), 1466–1478. https://doi.org/10.1021/acs.molpharmaceut.3c01106

Barba, A. A., d'Amore, M., Chirico, S., Lamberti, G., & Titomanlio, G. (2009). Swelling of cellulose derivative (HPMC) matrix systems for drug delivery. *Carbohydrate Polymers, 78*(3), 469–474. https://doi.org/10.1016/j.carbpol.2009.05.001

Bhujbal, S. V., Su, Y., Pathak, V., Zemlyanov, D. Y., Cavallaro, A. A., Munson, E. J., Taylor, L. S., & Zhou, Q. (2021). Effect of storage humidity on physical stability of spray-dried naproxen amorphous solid dispersions with polyvinylpyrrolidone: Two fluid nozzle vs. three fluid nozzle. Pharmaceutics, 13(7), 1–15. doi:https://doi.org/10.3390/PHARMACEUTICS13071074.

Bin, C., Joshi, S. C., & Lam, Y. C. (2009). Bio-fluid uptake and release of indomethacin of direct-compressed HPMC tablets. *Carbohydrate Polymers, 75*(2), 282–286. https://doi.org/10.1016/j.carbpol.2008.07.025

Caccavo, D., Lamberti, G., Barba, A. A., Abrahmsén-Alami, S., Viridén, A., & Larsson, A. (2017). Effects of HPMC substituent pattern on water up-take, polymer and drug release: An experimental and modelling study. *International Journal of Pharmaceutics, 528*(1–2), 705–713. https://doi.org/10.1016/j.ijpharm.2017.06.064

Chang, Y., Hu, C., Yang, R., He, D., Wang, X., Ning, B., … Sun, C. (2020). A Raman imaging-based technique to assess HPMC substituent contents and their effects on the drug release of commercial extended-release tablets. *Carbohydrate Polymers, 244* (May), Article 116460. https://doi.org/10.1016/j.carbpol.2020.116460

Chen, H., Pui, Y., Liu, C., Chen, Z., Su, C. C., Hageman, M., … Qian, F. (2018). Moisture-induced amorphous phase separation of amorphous solid dispersions: Molecular mechanism, microstructure, and its impact on dissolution performance. *Journal of Pharmaceutical Sciences, 107*(1), 317–326. https://doi.org/10.1016/j.xphs.2017.10.028

Cichosz, S., & Masek, A. (2020). IR study on cellulose with the varied moisture contents: Insight into the supramolecular structure. *Materials, 13*(20), 1–22. https://doi.org/10.3390/ma13204573

Deac, A., Qi, Q., Indulkar, A. S., Purohit, H. S., Gao, Y., Zhang, G. G. Z., & Taylor, L. S. (2023). Dissolution mechanisms of amorphous solid dispersions: Role of drug load and molecular interactions. *Molecular Pharmaceutics, 20*(1), 722–737. https://doi.org/10.1021/acs.molpharmaceut.2c00892

Deshmukh, S., Paradkar, A., Abrahmsén-Alami, S., Govender, R., Viridén, A., Winge, F., … Kelly, A. (2020). Injection moulded controlled release amorphous solid dispersions: Synchronized drug and polymer release for robust performance. *International Journal of Pharmaceutics, 575*(November 2019), Article 118908. https://doi.org/10.1016/j.ijpharm.2019.118908

Fan, N., He, Z., Ma, P., Wang, X., Li, C., Sun, J., … Li, J. (2018). Impact of HPMC on inhibiting crystallization and improving permeability of curcumin amorphous solid dispersions. *Carbohydrate Polymers, 181*(December 2017), 543–550. https://doi.org/10.1016/j.carbpol.2017.12.004

Feng, X., Vo, A., Patil, H., Tiwari, R. V., Alshetaili, A. S., Pimparade, M. B., & Repka, M. A. (2016). The effects of polymer carrier, hot melt extrusion process and downstream processing parameters on the moisture sorption properties of amorphous solid dispersions. *Journal of Pharmacy and Pharmacology, 68*(5), 692–704. https://doi.org/10.1111/jphp.12488

Gordon, M., & Taylor, J. S. (1952). Ideal copolymers and the second-order transitions of synthetic rubbers. i. Non-crystalline copolymers. *Journal of Applied Chemistry, 2*(9), 493–500. https://doi.org/10.1002/jctb.5010020901

Govender, R., Kissi, E. O., Larsson, A., & Tho, I. (2021). Polymers in pharmaceutical additive manufacturing: A balancing act between printability and product performance. *Advanced Drug Delivery Reviews, 177*(0316), Article 113923. https://doi.org/10.1016/j.addr.2021.113923

Grdadolnik, J. (2002). ATR-FTIR spectroscopy: Its advantage and limitations. *Acta Chimica Slovenica, 49*(3), 631–642. https://acta-arhiv.chem-soc.si/49/49-3-631.pdf.

Guan, Q., Ma, Q., Zhao, Y., Jiang, X., Zhang, H., Liu, M., … Han, J. (2021). Cellulose derivatives as effective recrystallization inhibitor for ternary ritonavir solid dispersions: In vitro-in vivo evaluation. *Carbohydrate Polymers, 273*(August), Article 118562. https://doi.org/10.1016/j.carbpol.2021.118562

Gupta, S. S., Solanki, N., & Serajuddin, A. T. M. (2016). Investigation of thermal and viscoelastic properties of polymers relevant to hot melt extrusion, IV: Affinisol™ HPMC HME polymers. *AAPS PharmSciTech, 17*(1), 148–157. https://doi.org/10.1208/s12249-015-0426-6

Ha, D. H., Ha, E. S., Park, H., Lee, S. K., Jeong, J. S., Kang, H. T., … Kim, M. S. (2025). Enhanced oral bioavailability of pranlukast by preparing amorphous solid dispersion via hot-melt extrusion. *Journal of Pharmaceutical Investigation, 55*(6), 837–852. https://doi.org/10.1007/s40005-024-00724-4

Haku, R., Suzuki, N., Ohashi, K., Titapiwatanakun, V., & Fukami, T. (2025). Nanogram-scale screening of amorphous solid dispersion and its stability with monitoring phase transition using low-frequency Raman spectroscopy. *Journal of Drug Delivery Science and Technology, 112*(July), Article 107237. https://doi.org/10.1016/j.jddst.2025.107237

Hancock, B. C., Shamblin, S. L., & Zografi, G. (1995). Molecular mobility of amorphous pharmaceutical solids below their glass transition temperatures. In *Pharmaceutical Research* (Vol. 12, issue 6, pp. 799–806). doi:https://doi.org/10.1023/A:1016292416526.

Huang, S., O'Donnell, K. P., Keen, J. M., Rickard, M. A., McGinity, J. W., & Williams, R. O. (2016). A new Extrudable form of Hypromellose: AFFINISOL™ HPMC HME. *AAPS PharmSciTech, 17*(1), 106–119. https://doi.org/10.1208/s12249-015-0395-9

Iemtsev, A., Hassouna, F., Mathers, A., Klajmon, M., Dendisová, M., Malinová, L., … Fulem, M. (2020). Physical stability of hydroxypropyl methylcellulose-based amorphous solid dispersions: Experimental and computational study. *International Journal of Pharmaceutics, 589*(September), Article 119845. https://doi.org/10.1016/j.ijpharm.2020.119845

Iyer, R., Jovanovska, V. P., Berginc, K., Jaklič, M., Fabiani, F., Harlacher, C., … Sanchez-Felix, M. V. (2021). Amorphous solid dispersions (ASDs): The influence of material properties, manufacturing processes and analytical technologies in drug product development. *Pharmaceutics, 13*(10). https://doi.org/10.3390/pharmaceutics13101682

Jin, C., Wu, F., Hong, Y., Shen, L., Lin, X., Zhao, L., & Feng, Y. (2023). Updates on applications of low-viscosity grade Hydroxypropyl methylcellulose in coprocessing for improvement of physical properties of pharmaceutical powders. *Carbohydrate Polymers, 311*(February), Article 120731. https://doi.org/10.1016/j.carbpol.2023.120731

Kalogeras, I. M., & Brostow, W. (2009). Glass transition temperatures in binary polymer blends. *Journal of Polymer Science Part B: Polymer Physics, 47*(1), 80–95. https://doi.org/10.1002/polb.21616

Kalutskaya, E. P., & Gusev, S. S. (1980). An infrared spectroscopic investigation of the hydration of cellulose. *Polymer Science U.S.S.R., 22*(3), 550–556. https://doi.org/10.1016/0032-3950(80)90378-0

Keßler, L., Mishra, R., Hietala, S., Lammens, M., Peltonen, L., Rades, T., … Luxenhofer, R. (2025). Amorphous solid dispersions of amphiphilic polymer excipients and indomethacin prepared by hot melt extrusion. *European Journal of Pharmaceutical Sciences, 204*(August 2024). https://doi.org/10.1016/j.ejps.2024.106960

Kissi, E. O., Nilsson, R., Nogueira, L. P., Larsson, A., & Tho, I. (2021). Influence of drug load on the printability and solid-state properties of 3D-printed naproxen-based amorphous solid dispersion. *Molecules, 26*(15). https://doi.org/10.3390/molecules26154492

Konno, H., & Taylor, L. S. (2008). Ability of different polymers to inhibit the crystallization of amorphous felodipine in the presence of moisture. *Pharmaceutical Research, 25*(4), 969–978. https://doi.org/10.1007/s11095-007-9331-3

Larsen, B. S., Kissi, E., Nogueira, L. P., Genina, N., & Tho, I. (2024). Impact of drug load and polymer molecular weight on the 3D microstructure of printed tablets. *European Journal of Pharmaceutical Sciences, 192*(October 2023). https://doi.org/10.1016/j.ejps.2023.106619

Larsson, M., Viridén, A., Stading, M., & Larsson, A. (2010). The influence of HPMC substitution pattern on solid-state properties. *Carbohydrate Polymers, 82*(4), 1074–1081. https://doi.org/10.1016/j.carbpol.2010.06.030

Li, B., Konecke, S., Wegiel, L. A., Taylor, L. S., & Edgar, K. J. (2013). Both solubility and chemical stability of curcumin are enhanced by solid dispersion in cellulose derivative matrices. *Carbohydrate Polymers, 98*(1), 1108–1116. https://doi.org/10.1016/j.carbpol.2013.07.017

Li, J., Hubert, M., Pinnamaneni, S., Tao, L., Zhao, J., Sharif, S., … Nazarenko, S. (2020). Effect of moisture sorption on free volume and relaxation of spray dried dispersions: Relation to drug recrystallization. *Journal of Pharmaceutical Sciences, 109*(2), 1050–1058. https://doi.org/10.1016/j.xphs.2019.10.018

Li, J., Wang, Y., & Yu, D. (2023). Effects of additives on the physical stability and dissolution of polymeric amorphous solid dispersions: A review. AAPS PharmSciTech, 24(7), 1–15. doi:https://doi.org/10.1208/s12249-023-02622-8.

Lin, X., Hu, Y., Liu, L., Su, L., Li, N., Yu, J., … Yang, Z. (2018). Physical stability of amorphous solid dispersions: A physicochemical perspective with thermodynamic, kinetic and environmental aspects. *Pharmaceutical Research, 35*(6). https://doi.org/10.1007/s11095-018-2408-3

Liu, X., Zhou, L., & Zhang, F. (2017). Reactive melt extrusion to improve the dissolution performance and physical stability of naproxen amorphous solid dispersions. *Molecular Pharmaceutics, 14*(3), 658–673. https://doi.org/10.1021/acs.molpharmaceut.6b00960

Löbmann, K., Laitinen, R., Grohganz, H., Gordon, K. C., Strachan, C., & Rades, T. (2011). Coamorphous drug systems: Enhanced physical stability and dissolution rate of indomethacin and naproxen. *Molecular Pharmaceutics, 8*(5), 1919–1928. https://doi.org/10.1021/mp2002973

Löbmann, K., Laitinen, R., Grohganz, H., Strachan, C., Rades, T., & Gordon, K. C. (2013). A theoretical and spectroscopic study of co-amorphous naproxen and indomethacin. *International Journal of Pharmaceutics, 453*(1), 80–87. https://doi.org/10.1016/j.ijpharm.2012.05.016

Marsac, P. J., Konno, H., Rumondor, A. C. F., & Taylor, L. S. (2008). Recrystallization of nifedipine and felodipine from amorphous molecular level solid dispersions containing poly(vinylpyrrolidone) and sorbed water. *Pharmaceutical Research, 25*(3), 647–656. https://doi.org/10.1007/s11095-007-9420-3

Marsac, P. J., Rumondor, A. C. F., Nivens, D. E., Kestur, U. S., Stanciu, L., & Taylor, L. S. (2010). Effect of temperature and moisture on the miscibility of amorphous dispersions of felodipine and poly(vinyl pyrrolidone). *Journal of Pharmaceutical Sciences, 99*(1), 169–185. https://doi.org/10.1002/jps.21809

Menges, F. (2022). Spectragryph - optical spectroscopy software. Version 1.2.16.1 http://www.effemm2.de/spectragryph/.

Mora-Castaño, G., Millán-Jiménez, M., Niederquell, A., Schönenberger, M., Shojaie, F., Kuentz, M., & Caraballo, I. (2024). Amorphous solid dispersion of a binary formulation with felodipine and HPMC for 3D printed floating tablets. *International Journal of Pharmaceutics, 658*(March). https://doi.org/10.1016/j.ijpharm.2024.124215

Moseson, D. E., & Taylor, L. S. (2023). Crystallinity: A complex critical quality attribute of amorphous solid dispersions. *Molecular Pharmaceutics, 20*(10), 4802–4825. https://doi.org/10.1021/acs.molpharmaceut.3c00526

O'Connell, P., Yoon, J. H., Geever, L. M., Kumar, D., Healy, A. M., & Serrano, D. R. (2025). Accelerated predictive stability (APS) strategies applied to screening pharmaceutical formulations: A comparison of spray dried and hot melt extruded nifedipine amorphous solid dispersions. *International Journal of Pharmaceutics, 683*(July), Article 126012. https://doi.org/10.1016/j.ijpharm.2025.126012

Oh, S. Y., Yoo, D. I., Shin, Y., & Seo, G. (2005). FTIR analysis of cellulose treated with sodium hydroxide and carbon dioxide. *Carbohydrate Research, 340*(3), 417–428. https://doi.org/10.1016/j.carres.2004.11.027

Otoni, C. G., Lorevice, M. V., Moura, M. R.d., & Mattoso, L. H. C. (2018). On the effects of hydroxyl substitution degree and molecular weight on mechanical and water barrier properties of hydroxypropyl methylcellulose films. *Carbohydrate Polymers, 185*(January), 105–111. https://doi.org/10.1016/j.carbpol.2018.01.016

Pajzderska, A., Mielcarek, J., & Wąsicki, J. (2022). The physical stability of Felodipine and its recrystallization from an amorphous solid dispersion studied by NMR Relaxometry. AAPS PharmSciTech, 23(4), 1–10. doi:https://doi.org/10.1208/s12249-022-02234-8.

Patil, H., Vemula, S. K., Narala, S., Lakkala, P., Munnangi, S. R., Narala, N., Jara, M. O., Williams, R. O., Terefe, H., & Repka, M. A. (2024). Hot-melt extrusion: From theory to application in pharmaceutical formulation—Where are we now? AAPS PharmSciTech, 25(2), 1–25. doi:https://doi.org/10.1208/s12249-024-02749-2.

Paudel, A., & Van Den Mooter, G. (2012). Influence of solvent composition on the miscibility and physical stability of naproxen/PVP K 25 solid dispersions prepared by cosolvent spray-drying. *Pharmaceutical Research, 29*(1), 251–270. https://doi.org/10.1007/s11095-011-0539-x

Paudel, A., Van Humbeeck, J., & Van Den Mooter, G. (2010). Theoretical and experimental investigation on the solid solubility and miscibility of naproxen in poly (vinylpyrrolidone). *Molecular Pharmaceutics, 7*(4), 1133–1148. https://doi.org/10.1021/mp100013p

Péter-Haraszti, A., Záhonyi, P., Farkas, A., Csontos, I., Nagy, Z. K., Szabó, E., den Mooter, G. Van, & Marosi, G. (2024). Thermal investigation of relaxations of interacting and non-interacting amorphous solid dispersions. Journal of Thermal Analysis and Calorimetry, 149(15), 8067–8083. doi:https://doi.org/10.1007/s10973-024-13281-7.

Prasad, E., Islam, M. T., Goodwin, D. J., Megarry, A. J., Halbert, G. W., Florence, A. J., & Robertson, J. (2019). Development of a hot-melt extrusion (HME) process to produce drug loaded Affinisol™ 15LV filaments for fused filament fabrication (FFF) 3D printing. *Additive Manufacturing, 29*(July), 100776. https://doi.org/10.1016/j.addma.2019.06.027

Pugliese, A., Toresco, M., Mcnamara, D., Iuga, D., Abraham, A., Tobyn, M., … Blanc, F. (2021). Drug-polymer interactions in acetaminophen/Hydroxypropylmethylcellulose acetyl succinate amorphous solid dispersions revealed by multidimensional multinuclear solid-state NMR spectroscopy. *Molecular Pharmaceutics, 18*(9), 3519–3531. https://doi.org/10.1021/acs.molpharmaceut.1c00427

Purohit, H. S., & Taylor, L. S. (2015). Phase separation kinetics in amorphous solid dispersions upon exposure to water. *Molecular Pharmaceutics, 12*(5), 1623–1635. https://doi.org/10.1021/acs.molpharmaceut.5b00041

Purohit, H. S., & Taylor, L. S. (2017). Phase behavior of ritonavir amorphous solid dispersions during hydration and dissolution. *Pharmaceutical Research, 34*(12), 2842–2861. https://doi.org/10.1007/s11095-017-2265-5

Riekes, M. K., Kuminek, G., Rauber, G. S., De Campos, C. E. M., Bortoluzzi, A. J., & Stulzer, H. K. (2014). HPMC as a potential enhancer of nimodipine biopharmaceutical properties via ball-milled solid dispersions. *Carbohydrate Polymers, 99*, 474–482. https://doi.org/10.1016/j.carbpol.2013.08.046

Rumondor, A. C. F., Marsac, P. J., Stanford, L. A., & Taylor, L. S. (2009). Phase behavior of poly(vinylpyrrolidone) containing amorphous solid dispersions in the presence of moisture. *Molecular Pharmaceutics, 6*(5), 1492–1505. https://doi.org/10.1021/mp900050c

Rumondor, A. C. F., Stanford, L. A., & Taylor, L. S. (2009). Effects of polymer type and storage relative humidity on the kinetics of felodipine crystallization from amorphous solid dispersions. *Pharmaceutical Research, 26*(12), 2599–2606. https://doi.org/10.1007/s11095-009-9974-3

Rumondor, A. C. F., Wikström, H., Van Eerdenbrugh, B., & Taylor, L. S. (2011). Understanding the tendency of amorphous solid dispersions to undergo amorphous-amorphous phase separation in the presence of absorbed moisture. *AAPS PharmSciTech, 12*(4), 1209–1219. https://doi.org/10.1208/s12249-011-9686-y

Sarabu, S., Kallakunta, V. R., Bandari, S., Batra, A., Bi, V., Durig, T., Zhang, F., & Repka, M. A. (2020). Hypromellose acetate succinate based amorphous solid dispersions via hot melt extrusion: Effect of drug physicochemical properties. Carbohydrate Polymers, 233(December 2019), 115828. doi:https://doi.org/10.1016/j.carbpol.2020.115828.

Sarode, A. L., Obara, S., Tanno, F. K., Sandhu, H., Iyer, R., & Shah, N. (2014). Stability assessment of hypromellose acetate succinate (HPMCAS) NF for application in hot melt extrusion (HME). *Carbohydrate Polymers, 101*(1), 146–153. https://doi.org/10.1016/j.carbpol.2013.09.017

Shi, Q., Li, F., Yeh, S., Wang, Y., & Xin, J. (2020). Physical stability of amorphous pharmaceutical solids: Nucleation, crystal growth, phase separation and effects of the polymers. *International Journal of Pharmaceutics, 590*(August), Article 119925. https://doi.org/10.1016/j.ijpharm.2020.119925

Svoboda, R., Nevyhoštěná, M., Macháčková, J., Vaculík, J., Knotková, K., Chromčíková, M., & Komersová, A. (2023). Thermal degradation of Affinisol HPMC: Optimum processing temperatures for hot melt extrusion and 3D printing. *Pharmaceutical Research, 40*(9), 2253–2268. https://doi.org/10.1007/s11095-023-03592-z

Taylor, L. S., & Zografi, G. (2025). From unwanted annoyances to Oral delivery saviors: The rollercoaster journey of amorphous drugs. *Molecular Pharmaceutics, 22*(9), 5125–5138. https://doi.org/10.1021/acs.molpharmaceut.5c00013

Tian, B., Zhang, L., Pan, Z., Gou, J., Zhang, Y., & Tang, X. (2014). A comparison of the effect of temperature and moisture on the solid dispersions: Aging and crystallization. *International Journal of Pharmaceutics, 475*(1), 385–392. https://doi.org/10.1016/j.ijpharm.2014.09.010

Viridén, A., Wittgren, B., & Larsson, A. (2009). Investigation of critical polymer properties for polymer release and swelling of HPMC matrix tablets. *European Journal of Pharmaceutical Sciences, 36*(2–3), 297–309. https://doi.org/10.1016/j.ejps.2008.10.021

Vlad, R. A., Pintea, A., Pintea, C., Rédai, E. M., Antonoaea, P., Bîrsan, M., & Ciurba, A. (2025). Hydroxypropyl methylcellulose—A key excipient in pharmaceutical drug delivery systems. *Pharmaceutics, 17*(6), Article 784. https://doi.org/10.3390/pharmaceutics17060784

Wang, Y., Rades, T., & Grohganz, H. (2023). Considerations on the kinetic processes in the preparation of ternary co-amorphous systems by milling. *Pharmaceutics, 15*(1). https://doi.org/10.3390/pharmaceutics15010172

Windbergs, M., Strachan, C. J., & Kleinebudde, P. (2009). Influence of the composition of glycerides on the solid-state behaviour and the dissolution profiles of solid lipid extrudates. *International Journal of Pharmaceutics, 381*(2), 184–191. https://doi.org/10.1016/j.ijpharm.2009.03.002

Wu, J., & Mooter, G. Van den. (2023). The influence of hydrogen bonding between different crystallization tendency drugs and PVPVA on the stability of amorphous solid dispersions. International Journal of Pharmaceutics, 646(September), 123440. doi:https://doi.org/10.1016/j.ijpharm.2023.123440.

Xie, T., & Taylor, L. S. (2017). Effect of temperature and moisture on the physical stability of binary and ternary amorphous solid dispersions of celecoxib. *Journal of Pharmaceutical Sciences, 106*(1), 100–110. https://doi.org/10.1016/j.xphs.2016.06.017

Yang, Z., Nollenberger, K., Albers, J., Moffat, J., Craig, D., & Qi, S. (2014). The effect of processing on the surface physical stability of amorphous solid dispersions. *European Journal of Pharmaceutics and Biopharmaceutics, 88*(3), 897–908. https://doi.org/10.1016/j.ejpb.2014.07.013

Yazdi, S., Benson, E., Taylor, L. S., & Edgar, K. J. (2025). Design and synthesis of cellulose ω-carboxythioalkyl alkanoate derivatives for amorphous solid dispersion of hydrophobic compounds. *Carbohydrate Polymers, 373*, Article 124669. https://doi.org/10.1016/j.carbpol.2025.124669

Zhang, J., Jiang, Q., Xu, Z., Yang, Q., Hao, G., Liu, M., & Zeng, Z. (2024). Recent Progress on crystal nucleation of amorphous solid dispersion. *Crystal Growth & Design*. https://doi.org/10.1021/acs.cgd.4c01114

Zhang, J., Shi, X., & Tao, W. (2023). Curcumin amorphous solid dispersions benefit from hydroxypropyl methylcellulose E50 to perform enhanced anti-inflammatory effects.

International Journal of Biological Macromolecules, 252(June), Article 126507. https://doi.org/10.1016/j.ijbiomac.2023.126507

Zhang, J., Yang, W., Vo, A. Q., Feng, X., Ye, X., Kim, D. W., & Repka, M. A. (2017). Hydroxypropyl methylcellulose-based controlled release dosage by melt extrusion and 3D printing: Structure and drug release correlation. *Carbohydrate Polymers, 177*(June), 49–57. https://doi.org/10.1016/j.carbpol.2017.08.058

Zhang, S., Lee, T. W. Y., & Chow, A. H. L. (2019). Thermodynamic and kinetic evaluation of the impact of polymer excipients on storage stability of amorphous itraconazole. *International Journal of Pharmaceutics, 555*(August 2018), 394–403. https://doi.org/10.1016/j.ijpharm.2018.11.063

Zhang, X., Luo, P., Wang, J., Yang, L., Pang, Z., Chen, S., … Qin, L. (2025). The comparison of anticrystallization effects of cellulose derivatives with polyvinylpyrrolidone and poloxamer on andrographolide: In vitro and in vivo characterization. *Carbohydrate Polymers, 358*(March), Article 123510. https://doi.org/10.1016/j.carbpol.2025.123510

Zhao, P., Wang, H., Jia, J., Song, D., Yang, L., Tang, X., … Fu, Q. (2024). Moisture-induced limited recrystallization may not reduce the dissolution of amorphous solid dispersions: A case of nitrendipine. *Journal of Industrial and Engineering Chemistry, 137*(August 2023), 235–242. https://doi.org/10.1016/j.jiec.2024.03.009